SciEn

Proceedings of 8th International Conference on Mechanical Engineering and Renewable Energy 2025
10-12 December, 2025, Chattogram, BANGLADESH

SciEn Conference Series: Engineering Vol. 4, 2026, pp 259-264 https://doi.org/10.38032/scse.2026.4.129

Brownian Motion and Thermophoresis Effects on Boundary Layer Nanofluid Flow over an Inclined Porous Surface with Mass Flux Condition

Joy Dev, Mohammad Ali, Umme Hani, and Muhammad Shahnewaz Bhuyan*

Department of Mathematics, Chittagong University of Engineering & Technology, Bangladesh

ABSTRACT

The current study intends to investigate thermophoresis and Brownian motion effects on boundary layer (BL) flow of nanofluid over an inclined porous stretched surface with a mass flux condition. The governing partial differential equations (PDEs) are converted into non-dimensional ordinary differential equations (ODEs) through an appropriate similarity transformation. The resulting equations are then solved using the Spectral Quasi-linearization method. Graphical representations illustrating the consequence of Brownian motion, Grashof number, thermophoresis, mass Grashof number, and suction/injection on velocity, temperature, and nanoparticle concentration are examined and discussed. The results indicated that an increase in Grashof number, mass Grashof number and thermophoresis parameter leads to the increase in the rate of fluid flow while it decreases when suction factor is increased within the boundary layer region. The influence of Brownian motion and thermophoresis parameter on nanoparticles improved the temperature profile but mass Grashof number and Grashof number decrease the temperature profile within the boundary layer region. However, the concentration profiles decrease up to certain values of eta, then increase for the thermophoresis parameter. In contrast, the Brownian motion parameter exhibits reverse trends. The present work has significant implications for various engineering applications, particularly in cooling systems and material processing. Understanding these effects can lead to enhanced performance in heat transfer mechanisms and improved efficiency in fluid dynamics.

Keywords: Brownian Motion, Buongiorno Model, Thermophoresis, Nanofluid, Porous Medium.

1. Introduction

Papers Nowadays, the development of nanotechnology has led to innovation in nanostructures, which are characterized by their exploratory usage in a range of biological applications. Developments in thermal engineering, nanoscience, and nanotechnology over the past few decades have led to the multidisciplinary field of nanofluid technology. Biotechnology, aerospace, information technology, the plastics and textile industries, food and agriculture, energy and the environment, cosmetics, health and medicine are just a few of the industries that could benefit from the novel features found in nanofluids. Because of its significance in the fields of industry, engineering, and pharmaceutical firms, nanofluids are currently a hot topic for research. These liquids are a blend of ordinary liquids and particles as small as nanometers. Choi [1] called these nanoliquids because of the incorporation of nanoparticles. He found that these elements are better at transferring energy than ordinary liquids, which lowers a heat transfer system's pumping cost by a number of times. Buongiorno [2] studied that Brownian motion and thermophoresis are the main heat transfer characteristics among other factors. Rafique et al. [3] have investigated the effects of mixed convection using nanoliquid for the Riga plate. To get results, they used the numerical technique. Additionally, the hybrid nanoliquid flow with the addition of second-order velocity slip was examined by Abu Bakar et al. [4]. The potential improvements in heat transfer efficiency made possible by the complementary interactions of magnetic fields and nanofluids in porous media settings were investigated by Bansal et al. [5]. Furthermore, research conducted by various academics [6 – 12] can be used to assess the significance of the thermal radiation influences on the flow caused by expanding sheets. To the best of knowledge, not much study has been done on nanofluid across inclined stretching surfaces while accounting for Brownian motion and thermophoresis incorporating mass flux condition. So, motivated by the foregoing explanation, the current study intends to investigate Brownian motion and thermophoresis effects on BL flow of nanofluid over an inclined porous stretched surface with a mass flux circumstance.

2. Mathematical Formulation

Consider the two-dimensional steady, viscous, incompressible nanofluid flows is passing an inclined porous plate in surrounding porous medium. In addition, the magnetic field (B_0) is introduced normal to the nanofluid flow direction. The two-dimensional coordinates x and y are along and normal direction of flow system. The velocity components of these flow directions are u and v respectively. The free stream velocity (U_∞), temperature (T_∞), and nanoparticle fraction (C_∞) of the flow field are assumed to be constant values in the surrounding environment, the angle to the vertical porous plate by α, and the gravity due to acceleration by g. It is assumed that the porous material has a constant magnetic field (B_0) and is uniform and isotropic. Furthermore, the wall concentration C_w is greater than the

ambient concentration C_∞, and the wall temperature T_w is greater than the ambient temperature T_∞.
As a result, the law of conservation of mass is automatically obeyed under the above-mentioned flow field considerations, as shown below.

$$\frac{\partial u}{\partial x}+\frac{\partial v}{\partial y}=0; \quad (1)$$

The modified dimensional BL equations such momentum, energy, and concentration equations for characterizing the nanofluid flow field can be stated as follows using the current physical features [5-7]:

Momentum Equation:

$$u\frac{\partial u}{\partial x}+v\frac{\partial u}{\partial y}=\nu\frac{\partial^2 u}{\partial y^2}+\left[\beta_T\left(T-T_\infty\right)+\beta_C\left(C-C_\infty\right)\right]g\cos\gamma-\frac{\nu}{k}u \quad (2)$$

Energy Equation:

$$u\frac{\partial T}{\partial x}+v\frac{\partial T}{\partial y}=\alpha\frac{\partial^2 T}{\partial y^2}+\tau\left[D_B\frac{\partial C}{\partial y}\frac{\partial T}{\partial y}+\frac{D_T}{T_\infty}\left(\frac{\partial T}{\partial y}\right)^2\right] \quad (3)$$

Nanoparticle Concentration Equation:

$$u\frac{\partial C}{\partial x}+v\frac{\partial C}{\partial y}=D_B\frac{\partial^2 C}{\partial y^2}+\frac{D_T}{T_\infty}\frac{\partial^2 T}{\partial y^2} \quad (4)$$

Boundary conditions are regarded in the following way.

$$\begin{gathered}u=U_w=ax^n, v=V_w, T=T_w(x)=T_\infty+Ax^n,\\ D_B\frac{\partial C}{\partial y}+\frac{D_T}{T_\infty}\frac{\partial T}{\partial y}=0 \text{ at y}=0\\ u\to 0, T\to T_\infty, C\to C_\infty \text{ as y}\to\infty\end{gathered} \quad (5)$$

Similarity Analysis

When incorporating the subsequent change and dimensionless quantities into equations, the boundary conditions are taken into consideration. In this regard, similarity transformation is introduced as follows:

$$\eta=y\sqrt{\frac{a(n+1)}{2\nu}}\,\mathrm{x}^{\mathrm{n-1}},\psi=\sqrt{2a\nu}\,x^{\frac{n+1}{2}}f(\eta),\theta(\eta)=\frac{T-T_\infty}{T_w-T_\infty}, \quad (6)$$
$$\phi(\eta)=\frac{C-C_\infty}{C_w-C_\infty},u=\frac{\partial\psi}{\partial y},v=-\frac{\partial\psi}{\partial x}$$

Method of solution

The continuity equation (1) satisfies equations (2 - 4) and transforms them as shown below. In order to solve the problem, the following ODEs are obtained by applying equation (6):

$$f'''(\eta)+f(\eta)f''(\eta)-\frac{(n+1)}{2n}f'^2(\eta)-\frac{2\lambda}{n+1}f'(\eta)+\frac{2}{n+1}(Gr\theta+Gm\phi)\cos\gamma=0 \quad (7)$$

$$\theta''(\eta)+\Pr\left(f(\eta)\theta'(\eta)-\frac{2n+1}{2n}f'(\eta)\theta(\eta)\right)+Nb\theta'(\eta)\phi'(\eta)+Nt\theta'^2(\eta)=0 \quad (8)$$

$$\theta''(\eta)+Le\left(f(\eta)\varphi'(\eta)-\frac{2n+1}{2n}f'(\eta)\varphi(\eta)\right)+\frac{Nt}{Nb}\phi''(\eta)=0 \quad (9)$$

Here

$$f_w=-\frac{V_w}{\sqrt{\nu a}},\lambda=\frac{\nu}{ak},\mathrm{Gr}=\frac{g\beta\left(T_w-T_\infty\right)}{a^2},\mathrm{Gm}=\frac{g\beta^*\left(C_w-C_\infty\right)}{a^2},$$
$$\Pr=\frac{\nu}{\alpha},Le=\frac{\nu}{\alpha},Nb=\frac{\tau D_B\left(C_w-C_\infty\right)}{\nu},Nt=\frac{\tau D_T\left(T_w-T_\infty\right)}{\nu}$$

The transformed boundary conditions are

$$\begin{gathered}f(\eta)=f_w, f'(\eta)=1,\theta(\eta)=1, Nb\varphi'(\eta)+Nt\theta'(\eta)=0 \text{ at } \eta=0\\ f(\eta)\to 0, f'(\eta)\to 0,\theta(\eta)\to 0,\varphi(\eta)\to 0, \text{ as } \eta\to\infty\end{gathered} \quad (10)$$

To find the numerical solution of the equations (7) - (9) with boundary equation (10), we have to follow the Chebyshev Spectral Collocation Method (CSCM) and the Quasi-Linearization method (QLM) are two numerical techniques that are combined to create the SQLM [13]. The Newton-Raphson based QLM was first put forth by [14]. It is employed to linearize the differential equation that is not linear into a series of linear differential equations that are iterative. The CSCM is used to integrate the resulting system of equations. The higher order ordinary differential equations (7) - (9) with boundary equation (10) into a system of first order ordinary differential equations in the following way:

Consider

$$f(\eta)=y_1, f'(\eta)=y_2, f''(\eta)=y_3,\theta(\eta)=y_4,$$
$$\theta'(\eta)=y_5,\varphi(\eta)=y_6,\varphi'(\eta)=y_7.$$

Therefore, the system of first order ordinary differential equations can be written as

$$\begin{aligned}
y_1'&=f'(\eta)=y_2\\
y_2'&=f''(\eta)=y_3\\
y_3'&=-y_1y_3+\frac{(n+1)}{2n}y_2^2+\frac{2\lambda}{n+1}y_2-\frac{2}{n+1}\left(Gry_4+Gmy_6\right)\cos\gamma\\
y_4'&=\theta'(\eta)=y_5\\
y_5'&=\Pr\left(y_1y_5-\frac{2n+1}{2n}y_2y_4\right)+Nby_5y_7+Nty_5^2\\
y_6'&=\varphi'(\eta)=y_7\\
y_7'&=-\frac{Nb}{Nt}Le\left(y_1y_7-\frac{2n+1}{2n}y_2y_6\right)-\frac{Nb}{Nt}\theta''(\eta)
\end{aligned}$$

The boundary conditions are converted as

$$\begin{gathered}y_1=f_w, y_2=1, y_2=1, Nby_7+Nty_5=0 \quad \text{at } \eta=0\\ y_2=y_4=y_6\to 0, \quad \text{as } \eta\to\infty\end{gathered}$$

3. Results and Discussion

Numerical computations of non-linear ODEs (7-9) having boundary conditions (10) are derived by applying the Spectral Quasi-Linearization method. The effects of several variables, including the suction parameter f_w, Brownian motion Nb, thermophoresis Nt, Grashof number Gr, mass Grashof number Gm, and inclination angle γ, are shown using graphs and tables. In this context, f'(η), θ(η), and $\phi(\eta)$ indicate the profiles' vertical axis with their accompanying legends, which correlate to velocity, temperature, and nanoparticle concentration, respectively, while η represents each case's horizontal axis. In the meantime, the legends showed how each setting affected the system. The following is a discussion of their effects on the flow:

3.1 Impact of suction parameter

The impact of the suction parameter f_w on the velocity profile $f'(\eta)$ is depicted in Figure 1(a), the $f'(\eta)$ decreases for the suction parameter f_w. The similar result has been observed for temperature $\theta(\eta)$ in Figure 1(b) i.e., the temperature decreases for f_w.

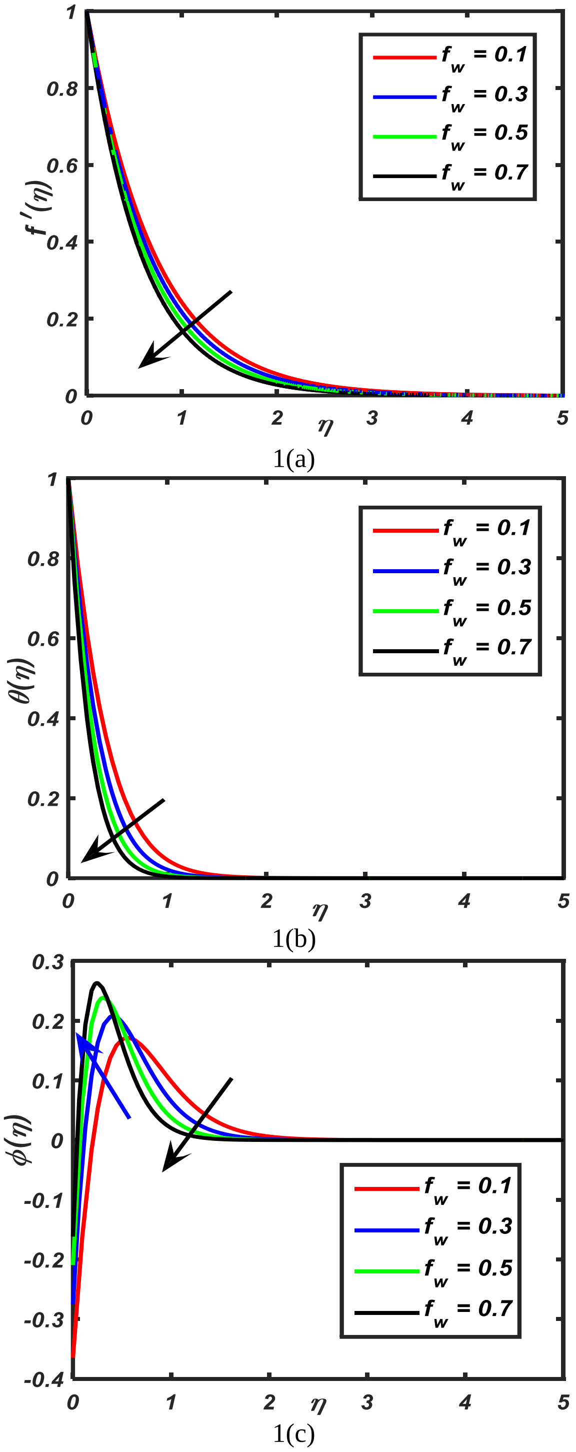

Fig.1: Impact of f_w on a) f', b) θ, and c) ϕ

On the other side, opposite effect is observed for nanoparticle concentration $\varphi(\eta)$ by increasing the suction parameter f_w shown in Figure 1(c). This type of behavior occurs when the fluid is drawn closer to the surface by suction, which thins the boundary layer and increases skin friction.

3.2 Impact of Grashof number

The consequence of Grashof number Gr on velocity profile $f'(\eta)$ elucidated in Figure 2(a). The intriguing outcome seen that velocity is dropping up, when the value of Gr boosts up. On the other side, opposite effect is observed for temperature $\theta(\eta)$ and nanoparticle concentration $\varphi(\eta)$ by increasing the Grashof number Gr shown in Figure 2(b) and 2(c) respectively. This type of behavior occurs when the fluid is drawn closer to the surface by suction, which thins the boundary layer and increases skin friction. This type of behavior occurs as a result of buoyancy forces, which are the main forces behind natural convection, increasing in magnitude with a larger Grashof number. As a result, the fluid flows more quickly, increasing the velocity profiles inside the fluid barrier layer. Electrical power is transformed into for Lorentz force, which increase the fluid's heat and mass. The overall fluid temperature rises close to the surface of an inclined surface as the angle increases because the convective heat transfer coefficient decreases. Since convection and flow patterns alter the diffusion and movement of species within the fluid, an upsurge in the inclination angle results an increment of concentration profile.

3.3 Impact of Mass Grashof number

The impact of mass Grashof number on f', θ, and ϕ are depicted in Figure 3(a) - 3(c).
Velocity profile increases but temperature and concentration decrease which are depicted in Figure 3(a) - 3(c). The Grashof number, which exemplifies the ratio of buoyant forces to viscous forces, is what causes this type of behavior. A greater mass Grashof number indicates that buoyancy is more prevalent, which strengthens the force propelling fluid motion and raises velocity. This is due to the fact that higher velocity brought about by stronger buoyant forces can dilute or lower concentration levels across a given area and temperature.

3.4 Impact of Brownian motion

The impacts of Nb on f', θ, and ϕ are depicted in Figure 4(a) - 4(c). It is noticed that velocity and temperature profiles are constant but nanoparticle concentration increases up to certain values of eta then decreases.

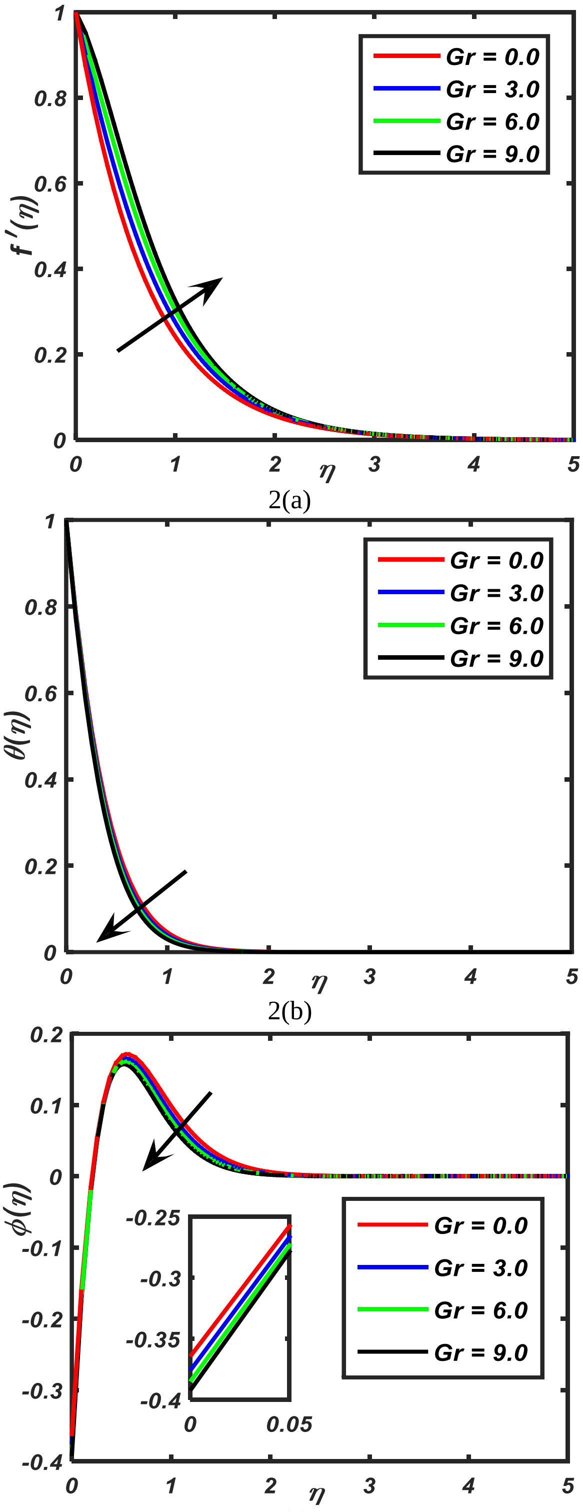

Fig. 2: Impact of Gr on a) f', b) θ, and c) ϕ.

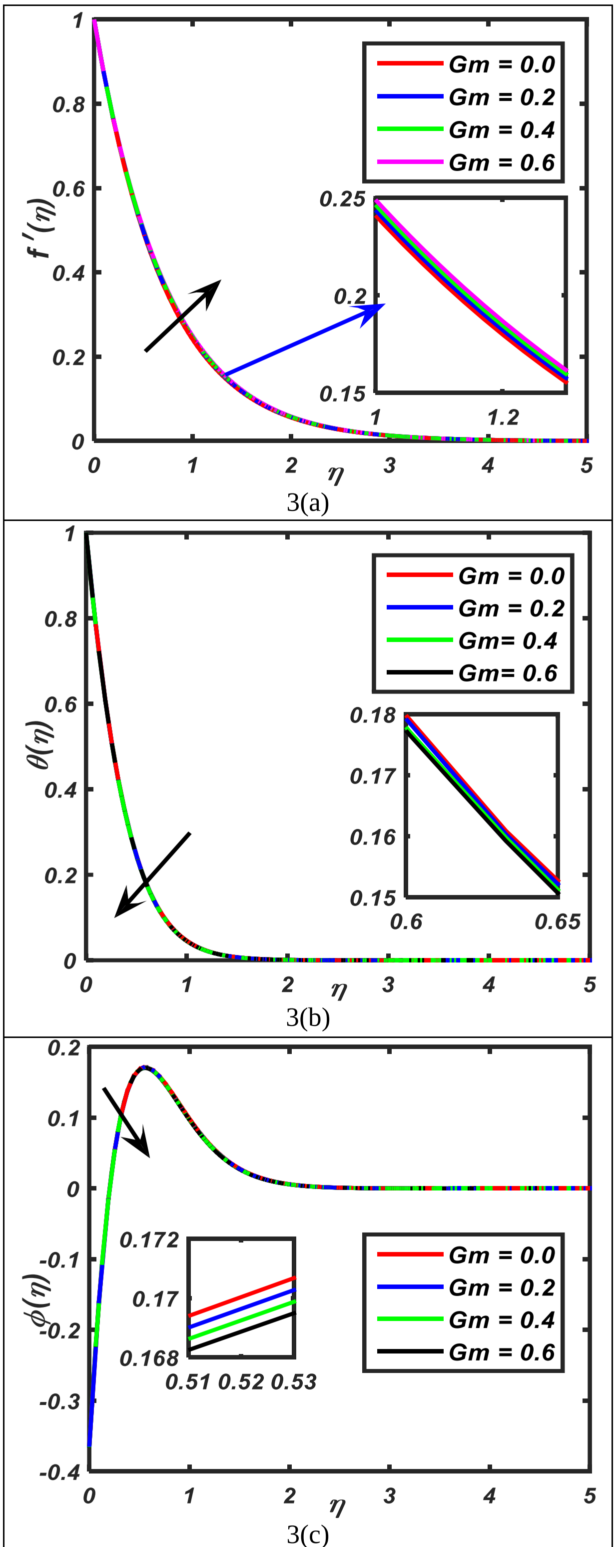

Fig. 3: Impact of Gm on a) f', b) θ, and c) ϕ.

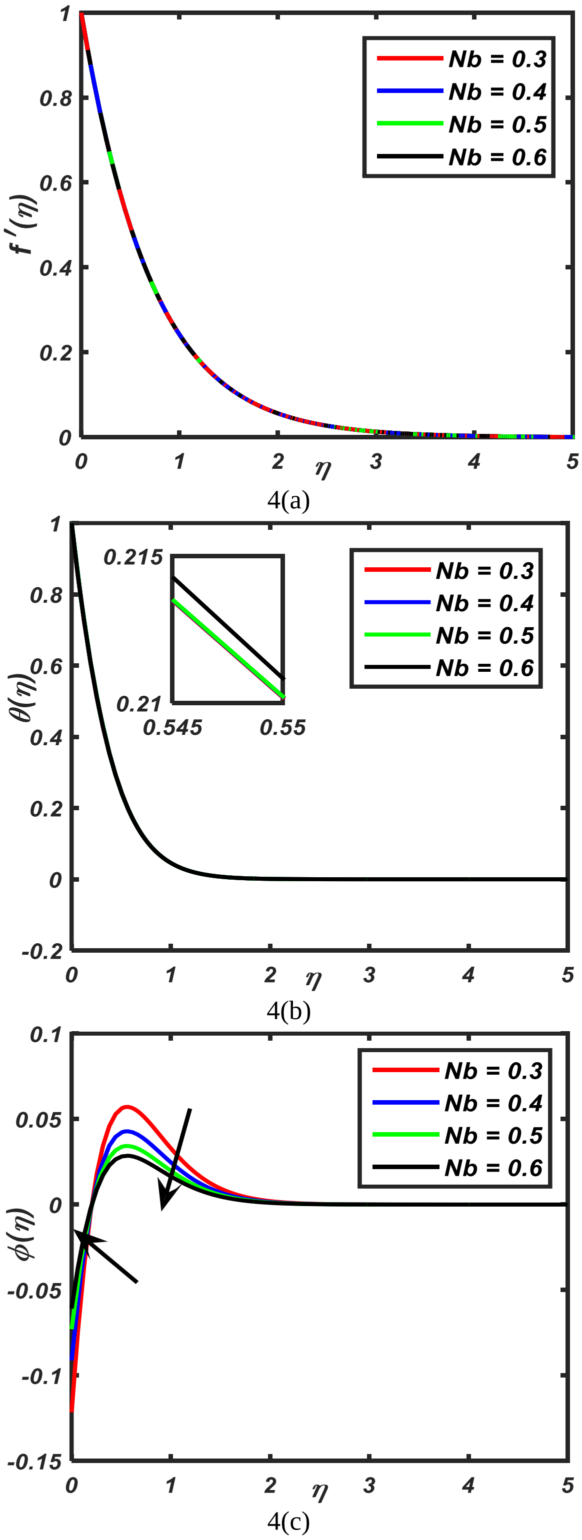

Fig. 4: Impact of Nb on a) a) f', b) θ, and c) ϕ.

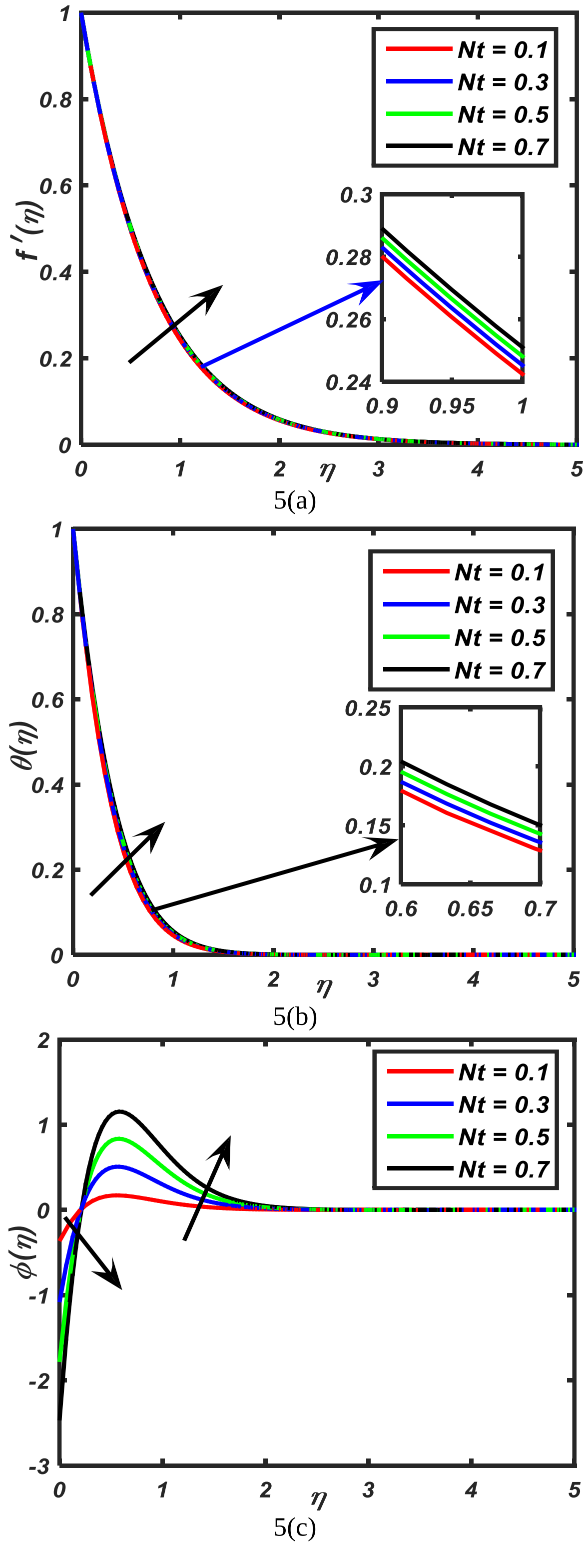

Fig. 5: Impact of Nt on a) f', b) θ, and c) ϕ.

3.5 Impact of Thermophoresis

The impacts of thermophoresis on f', θ, and $\phi$are depicted in Figure 5(a) - 5(c). Velocity and temperature profiles are increases but nanoparticle concentration decreases up to certain values of eta then increases. Small particles suspended in a fluid exposed to a temperature gradient experience a force that causes them to migrate from hotter to cooler regions, which is how thermophoresis affects velocity, temperature, and concentration distribution. Changes in velocity result from this, as the thermophoretic force pushes the particles, giving them a thermophoretic velocity.

4. Concluding Remark

In this study, we investigated the impact of Brownian motion and thermophoresis on the two-dimensional boundary layer nanofluid flow of the fluid towards an inclined sheet with mass flux condition. The consequence of concerned parameters on the velocity and temperature, and nanoparticle concentration profiles has been investigated.
The major findings of this study are summarized in the following way.

- The velocity profile is inversely proportional to suction parameter but directly proportional to Brownian motion, mass Grashof number, thermophoresis, and Grashof number.

- The temperature profile is inversely proportional to suction parameter, Brownian motion, Grashof number, and mass Grashof number but directly proportional to thermophoresis, parameter.
- The concentration profile is an increasing-decreasing function for the Brownian motion, suction parameter, and thermophoresis parameter but inversely proportional to Grashof number and mass Grashof number.

5. References

[1] Choi, S. U. and Eastman, J. A., 1995, January. Enhancing thermal conductivity of fluids with nanoparticles. *Argonne National Laoratory., IL United States* (No. ANL/MSD/CP-84938; CONF-951135-29).

[2] Buongiorno, J., 2006. Convective transport in nanofluids. *Journal of Heat Transf*er, 128(03), pp. 240-250. March.

[3] Rafique, K., Alotaibi, H., Ibrar, N. and Khan, I., 2022. Stratified flow of micropolar nanofluid over riga plate: Numerical analysis. *Energies*, 15(01), pp. 316.

[4] Bakar, S.A., Wahid, N.S., Arifin, N.M. and Khashi'ie, N.S., 2022. The flow of hybrid nanofluid past a permeable shrinking sheet in a Darcy–Forchheimer porous medium with second-order velocity slip. *Waves in Random and Compex. Media*, 35(04), pp. 1-18.

[5] Bansal, S., Pal, J., Bisht, M.S. and Fartyal P. 2024. Influence of nanofluids on boundary layer flow over an inclined stretching sheet in a porous media along with magnetic field. *International Journal of Mathematical, Engineering and Management Sciences*, 9(02), pp. 267-282.

[6] Nadeem, S., Fuzhang, W., Alharbi, F.M., Sajid, F., Abbas, N., El-Shafay, A.S. and Al-Mubaddel, F.S., 2022. Numerical computations for Buongiorno nanofluid model on the boundary layer flow of viscoelastic fluid towards a nonlinear stretching sheet. *Alexandria Engineering J*ournal, 61(02), pp. 1769-1778.

[7] Anwar, M.I., Shafie, S., Kasim, A.R.M. and Salleh, M.Z., 2016. Radiation effect on MHD stagnation-point flow of a nanofluid over a nonlinear stretching sheet with convective boundary condition. *Heat Transfer Research*, 47(09), pp. 797-816.

[8] Maleki, H., Alsarraf, J., Moghanizadeh, A., Hajabdollahi, H. and Safaei, M.R., 2019. Heat transfer and nanofluid flow over a porous plate with radiation and slip boundary conditions. *Journal of Central South University*, 26(05), pp. 1099-1115.

[9] Wang, F., Jamshed, W., Usman, Ibrahim, R.W., Abdalla, N.S.E., Abd-Elmonem, A. and Hussain, S.M., 2023. Solar radiative and chemical reactive influences on electromagnetic Maxwell nanofluid flow in Buongiorno model. *Journal of Magnetism and Magnetic Materials*, 576(04), pp. 170748.

[10] Mebarek-Oudina, F., Preeti, A.S., Sabu, H., Vaidya, R. Lewis, W., Areekara, S. and Ismail, A.I., 2024. Hydromagnetic flow of magnetite–water nanofluid utilizing adapted Buongiorno model. *International Journal of Modern Physics B*, 38(01), pp. 2450003.

[11] Areekara, S., Mackolil, J., Mahanthesh, B. and Mathew, A., 2022. Bulirsch-Stoer computations for bioconvective magnetized nanomaterial flow subjected to convective thermal heating and Stefan blowing: A revised Buongiorno model for theranostic applications. *Waves in Random and Complex Media*, *35*(5), pp. 9094-9126.

[12] Rafique, K., Anwar, M.I., Misiran, M., Khan, I., Seikh, A.H., Sherif, E.S.M. and Nisar K.S., 2019. Keller-box simulation for the Buongiorno mathematical model of micropolar nanofluid flow over a nonlinear inclined surface. *Processes*, 7(12), pp. 926.

[13] Muzara, H., Shateyi S. and Marewo, G.T., 2018. Spectral Quasi-Linearization Method for solving the Bratu problem. *Advances and Applications in Fluid Mechanics*, 21(04), pp. 449-463.

[14] Bellman, R.E. and Kalaba, R.E., 1965. Quasilinearization and Nonlinear Boundary-value Problems. *Elsevier*, *New York*.

6. Nomenclature

Symbol	Meaning	Unit
ODEs	Ordinary differential equations	-
u	Velocity component along x-axis	(ms^{-1})
v	Velocity component along y-axis	(ms^{-1})
σ	Electrical conductivity	(Sm^{-1})
υ	Kinematic viscosity	(kgm^{-3})
ρ	Density of fluid	(kgm^{-3})
α	Thermal diffusivity	(m^2s^{-1})
D_B	Brownian diffusion	(m^2/s)
D_T	Thermophoresis diffusion	(m^2/s)
k	Thermal conductivity	(W/(m·K))
h	Coefficient of heat transfer	($W/(m^2K)$)
τ	Ratio of nanoparticle effective and base fluid heat capacity	Dimensionless
f_w	Suction parameter	Dimensionless
Pr	Prandtl number	Dimensionless
Sc	Schmidt number	Dimensionless
Nb	Brownian motion parameter	Dimensionless
Nt	Thermophoresis parameter	Dimensionless
Gr	Grashof number	Dimensionless
Gm	Mass Grashof number	Dimensionless